

Optical Diagnostics of a Turbulent Pulverized Coal Combustion Flame

*Hirofumi TSUJI * , Seung min HWANG** , Fumiteru AKAMATSU**
Ryoichi KUROSE* , Hisao MAKINO* and Masashi KATSUKI***

** Energy Engineering Research Laboratory
Central Research Institute of Electric Power Industry (CRIEPI)
2-6-1 Nagasaka, Yokosuka, Kanagawa 240-0196, JAPAN
** Department of Mechanical Engineering, Osaka University
2-1 Yamada-oka, Suita, Osaka 565-0871, JAPAN*

ABSTRACT

The measurements of physical quantities in combustion fields based on optical diagnostics techniques, which allow non-invasive measurements of velocity, density, temperature, pressure and species concentration, have recently become of major interest as tools not only for clarifying the combustion mechanism but also for validating the computational results for the combustion fields. In this study, the combustion characteristics of a pulverized coal combustion flame are investigated using advanced optical diagnostics. A laboratory-scale pulverized coal combustion burner is specially fabricated. Velocity and shape of non-spherical pulverized coal particles and light emissions from a local point in the flame are measured by shadow Doppler particle analyzer (SDPA), and a specially designed receiving optics (multi-color integrated receiving optics, MICRO), respectively. The simultaneous measurement of OH planar laser-induced fluorescence (OH-PLIF) and Mie scattering image of pulverized coal particles is performed to examine spatial relation of combustion reaction zone and pulverized coal particle. The results show that the size-classified velocity and swelling of the pulverized coal particles in the flame can be observed by using SDPA. It is also found that the measurements of the OH chemiluminescence and CH band light emission from a local point in the flame using MICRO and the simultaneous instantaneous OH-PLIF and Mie scattering image of pulverized coal are effective for evaluating the ignition condition and characteristic of the pulverized coal combustion flames and for investigating their detailed flame structure.

Keywords : Pulverized coal combustion, SDPA, PLIF, Mie scattering

1. INTRODUCTION

Coal is an important and promising energy resource for electricity supply because its reserve is far more abundant than those of the other fossil fuels. For pulverized coal combustion, which has been mainly involved in coal-fired thermal power plants, it is desired to operate boilers with higher efficiency and lower pollutant emission, and recently to utilize various coals (i.e., low-rank coals) for diversifying fuel sources and lowering the cost in Japan. To efficiently develop new technologies for these requirements, it is of great importance to understand the pulverized coal combustion mechanism in detail. However, the combustion process of the pulverized coal is not well clarified so far, since it is a complex phenomenon, in which dispersion of coal particles, their devolatilization, chemical reactions of volatilized fuel and residual char with air, take place interactively at the same time and the simultaneous and instantaneous measurements for them are very difficult. Furthermore, though numerical simulation of the pulverized coal combustion has been performed as a supporting tool for the developments of the new technologies in these days (Kurose et al., 2004; Kurose et al., 2001a; Kurose et al., 2001b), its reliability has not been sufficiently confirmed yet because of the lack of the reliable detailed measured data to be compared with.

The measurements of physical quantities based on optical diagnostics techniques, which allow non-invasive measurements of velocity, density, temperature, pressure and species concentration, have recently become of major interest. The particle velocity has been measured in the pulverized coal combustion flame using laser Doppler velocimetry (LDV) (Schnell, 1993) in these days. However, LDV cannot provide detailed investigation on particle diameter change and size-classified particle velocity, because LDV measures overall velocity of pulverized coal particles with diameter distribution. For measuring particle velocity and size simultaneously, phase Doppler anemometer (PDA) is widely used nowadays. However, the application is limited to spherical particles. Maeda et al. (1997) and Hardalupas et al. (1994) developed shadow Doppler particle analyzer (SDPA) by extending the LDV system as a method for simultaneous measuring velocity and particle shape of non-spherical particles such as pulverized coal. On the other hand, light emissions and radicals such as OH, CH, NO and so on in the combustion fields have been monitored by a specially designed receiving optics (multi-color integrated receiving optics, MICRO) and a laser-induced fluorescence (LIF) to investigate chemical reaction in gas and oil combustion fields. Presently, LIF is extended to the planar LIF (PLIF) to visualize two-dimensional distribution with high temporal and spatial resolution (Rothe et al., 1997; Deguchi et al., 1997; Akamatsu et al., 1999).

The purpose of this study is to investigate the combustion characteristics of the pulverized coal combustion flame using advanced optical diagnostics in detail. A laboratory-scale pulverized coal combustion burner is specially fabricated. Velocity and shape of non-spherical pulverized coal particles and light emissions from a local point in the flame are measured by SDPA and MICRO, respectively. In addition, to examine spatial relation of combustion reaction zone and pulverized coal particle, the simultaneous measurement of OH-PLIF and Mie scattering image of pulverized coal particles is performed.

2. EXPERIMENTAL APPARATUS AND METHODS

A turbulent pulverized coal combustion burner and the supplying system of coal, air and methane are illustrated schematically in Fig. 1. The main air for combustion is supplied from a compressor and the flow rate is regulated by a mass-flow controller. Pulverized coal particles, supplied and regulated by a screw feeder, is sucked by the main air flow and mixed with the air in a injector to form solid-gas two phase jet issued from the main burner port (inner diameter : 6 mm). Methane is supplied to annular slit burner (width : 0.5 mm) installed outside of the central port to ignite the two-phase jet because the coal injection rate is very small and the flame stabilization is impossible for pure pulverized coal combustion flame. The burner is set up on a three-dimensional traverser for precise positioning in measurement, and confined in an acrylic duct with octagon section for isolating the flame from external disturbance. Eight quartz windows are equipped on sidewall of the duct for optical access for laser insertion, light detection and flame observation. The origin for measurement is located at the center of the burner port, and z and r denote the axial and radial distances from the origin, respectively.

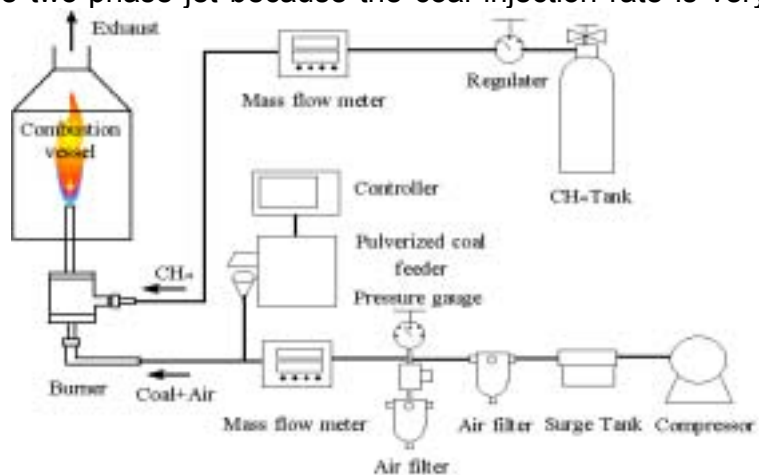


Fig. 1 Schematic diagram of a burner and a supply system of coal, air and methane

Tables 1 and 2 show the properties of used coal and the experimental condition, respectively. Coal we used is Newlands, and this is pulverized on the same condition for actual pulverized coal-fired thermal power plants. The mass base median diameter measured by a laser diffraction particle size analyzer is 33 μ m. The methane flow rate is the minimum amount to form stable flame. The pulverized coal is supplied after the methane diffusion flame became stable, and the measurement is started when the pulverized coal injection rate is regulated. Unburned pulverized coal particles in exhaust gas are collected by bag filters and exhaust gas is released into atmosphere by a ventilator after cooling by a heat exchanger.

Figure 2 shows the direct photograph of the pulverized coal combustion flame (exposure time : 1/8000 sec). The pulverized coal particles are visualized by an Ar-ion laser sheet inserted above the burner port. The photograph shows that the ignition of pulverized coal particles starts in the vicinity of the burner port of $z = 30$ mm and combustion proceeds

Table 1 Coal properties

High heating value ^{*1}	29.1 MJ/kg
Low heating value ^{*2}	28.1 MJ/kg
Proximate analysis	[wt %]
Moisture ^{*2}	2.60
Ash ^{*1}	15.20
Volatile matter ^{*1}	26.90
Fixed carbon ^{*1}	57.90
Ultimate analysis	[wt %]
Carbon ^{*1}	71.90
Hydrogen ^{*1}	4.40
Nitrogen ^{*1}	1.50
Oxygen ^{*1}	6.53
Total sulfur ^{*1}	0.44

Table 2 Experimental conditions

Pulverized coal feed rate	$1.49 \cdot 10^{-4}$ kg/s
Thermal input of coal	4.19 kW
Thermal input of methane	0.83 kW
Air flow rate	$1.83 \cdot 10^{-4}$ m ³ /s
Methane flow rate	$2.33 \cdot 10^{-4}$ m ³ /s
Bulk equivalence ratio	□□□□

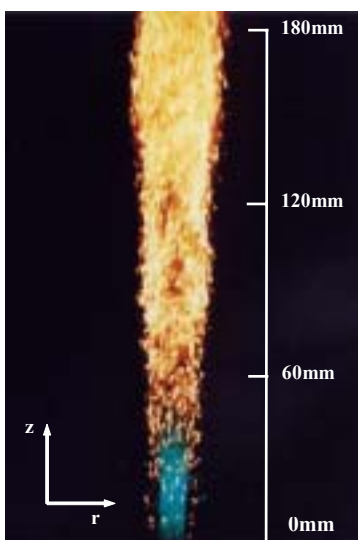


Fig. 2 Direct photograph of the pulverized coal combustion flame

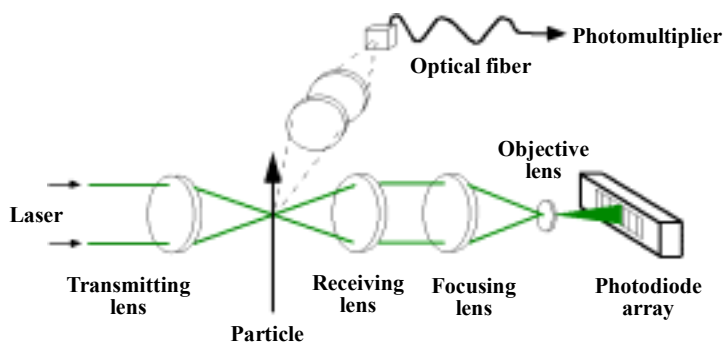


Fig. 3 Optical arrangement of SDPA

downstream to form luminous flame. Figure 3 shows the schematic diagram of SDPA. The SDPA is based on the imaging of a conventional LDV probe volume onto a linear photodiode array. The new aspect of this instrumentation is that the shape of the particles is obtained from the temporal output from elements of a linear photodiode array positioned at the focal plane of the collection optics of LDV to record the shadow of the passage of the particle. The detailed measurement principle is described in refs (Maeda et al., 1997; Rothe et al., 1997). The shape and two components of velocity of burning pulverized coal particles are measured in the turbulent pulverized coal combustion flame. Equivalent circle diameter is calculated from section area of each particle for size measurement.

The OH chemiluminescence (306 nm), CH band light emission (431.5 nm) and Mie scattering (514.5 nm) from a local point of pulverized coal combustion flame are measured by MICRO. The detailed optical system for local point measurement is described in ref (Akamatsu et al., 1999).

The simultaneous measurement system for OH-PLIF and Mie scattering image of pulverized coal particles is shown in Fig. 4. To illuminate the pulverized coal particles, a 2nd harmonic wave of Nd:YAG laser (Spectra-Physics, GCR-270-10) is used. For the OH-PLIF, P1 (8) absorption line (285.586nm) of (1,0) band is excited by using a wavelength tunable laser (Spectra-Physics, MOPO-730) pumped by a 3rd harmonic wave of the same Nd:YAG

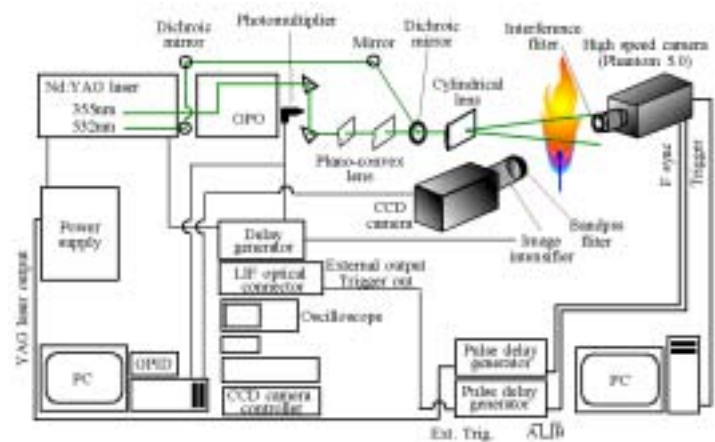


Fig. 4 Schematic apparatus of simultaneous measurement system for OH-PLIF and Mie scattering

laser. The two laser beams of the different wavelength are aligned in the same passage using a dichroic mirror and formed into a thin laser light sheet, approximately 1.5 mm thickness, illuminating a vertical plane including the central axis of the flame above the burner port.

Mie scattering of pulverized coal particles is passed through the optical bandpass interference filter with transmission peak wavelength of 532 nm and half value width of 1.0 nm, and is captured by a CCD camera (Vision Research Systems, Phantom Ver. 5.0). Laser induced OH fluorescence, on the other hand, is passed through the optical bandpass interference filter with transmission peak wavelength of 320 nm and half value width of 20 nm and captured by a CCD camera (Roper, Model EEV 02-06-202) coupled with an image intensifier.

The imaging area is a square of 30 mm by 30 mm located at around the central axis of the flame. TTL signals generated by two pulse delay generators (PDG) (Stanford Research Systems, Model DG535) are used for timing control of the Nd:YAG laser, and image capture of OH-PLIF and Mie scattering image of pulverized coal particles.

3. RESULTS AND DISCUSSION

3.1 Simultaneous measurement of velocity and shape of pulverized coal particles in flame by SDPA

In SDPA measurement, velocity is obtained only when the particle shape is measured correctly. Hence, the validity of velocity data obtained by SDPA is assessed by comparing

with LDV measurement. Figure 5 shows the axial distributions of mean and rms (root mean square) velocities of pulverized coal particles by SDPA and LDV, and mean diameter (equivalent circle diameter) by SDPA. It is found that the velocity data of SDPA is well consistent with that by LDV. This verifies that accuracy of velocity measurement by SDPA is the same level as LDV. Mean and rms velocity of particles decreases with increasing axial distance, z . Mean diameter of particles, on the other hand, increases with moving downstream.

Figures 6 shows the size-classified mean and rms axial velocities of pulverized coal particles at the distances from the burner of $z = 60, 120$ and 180 mm. The measurements are done on the center and edge of the flame jet. The mean and rms velocities of pulverized coal particles on the center ($r = 0$ mm) do not indicate significant change with particle diameter, whereas those on the edge increase with particle diameter. The reason for this is considered as follows. The particles in central high-speed region tend to be transferred to outside in radial direction owing to thermal expansion of gas phase and organized motions appeared in jet. Although the axial velocity of the small particles transferred outside is quickly decreased by the ambient fluid with lower velocity, that of the larger particles is not affected by the ambient fluid because of larger inertia. Therefore, the larger the particle size is, the higher the velocity of pulverized coal particle is on the edge.

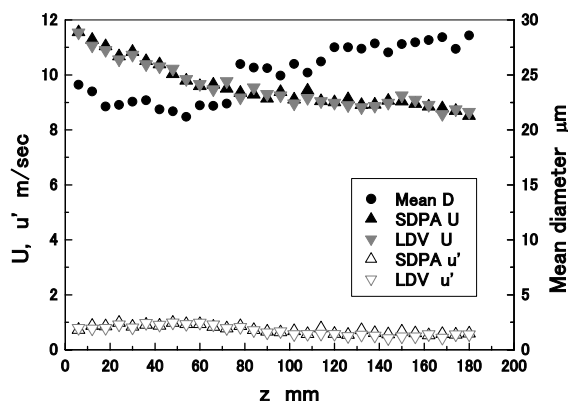
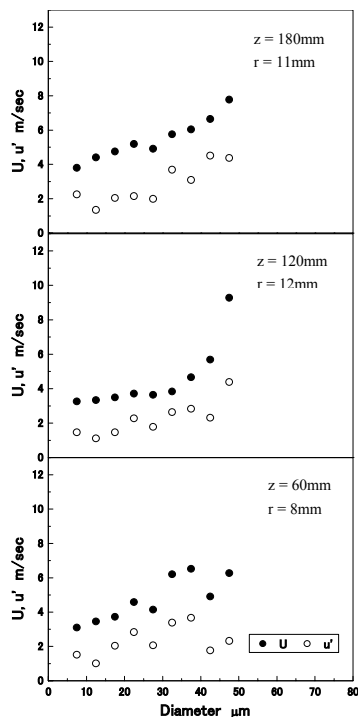
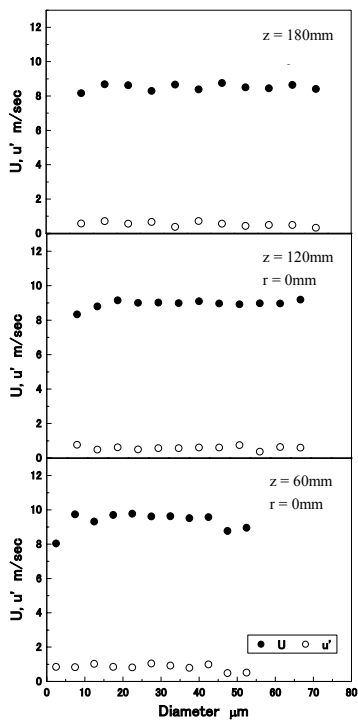


Fig. 5 Axial distributions of mean and rms (root mean square) velocities of coal particles by SDPA and LDV, and mean diameter by SDPA



(a) $z = 60, 120$ and 180 mm, center position (b) $z = 60, 120$ and 180 mm, edge position
Fig. 6 Mean and rms particle velocities for each $5\mu\text{m}$ particle size class

3.2 Local measurement of OH chemiluminescence and CH band light emission from flame and Mie scattering of pulverized coal particles by MICRO

Figure 7 shows the axial intensity profiles of OH chemiluminescence, CH band light emission and Mie scattering from a local point of pulverized coal particles by MICRO. Mie scattering intensity decreases with increasing the distance from burner due to the disappearance of pulverized coal particles in the flame. The intensity of OH chemiluminescence and CH band light emission shows the tendency to increase gradually, and finally decrease with going downstream. The reason for the high intensity of OH chemiluminescence near the burner exit ($z = 6 \sim 18\text{mm}$) is due to the effect of the pilot burner of methane diffusion flame. It is also found that the OH chemiluminescence and CH band light emission show high values at around $z = 80 \sim 120\text{mm}$, where the pulverized coal combustion actively takes place (see Fig. 2). Thus, it can be said that the measuring the light emissions' intensities is the effective method for evaluating the ignition condition and characteristic of the pulverized coal combustion flame.

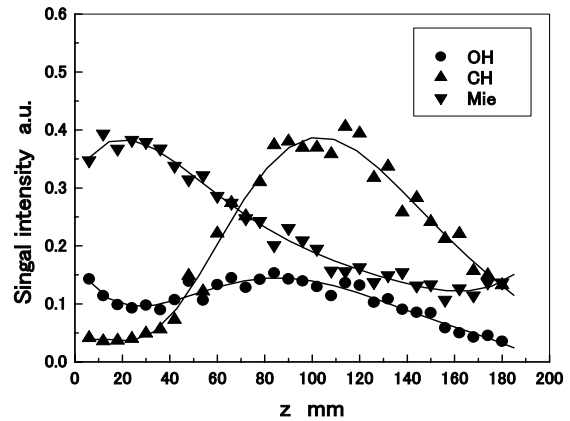
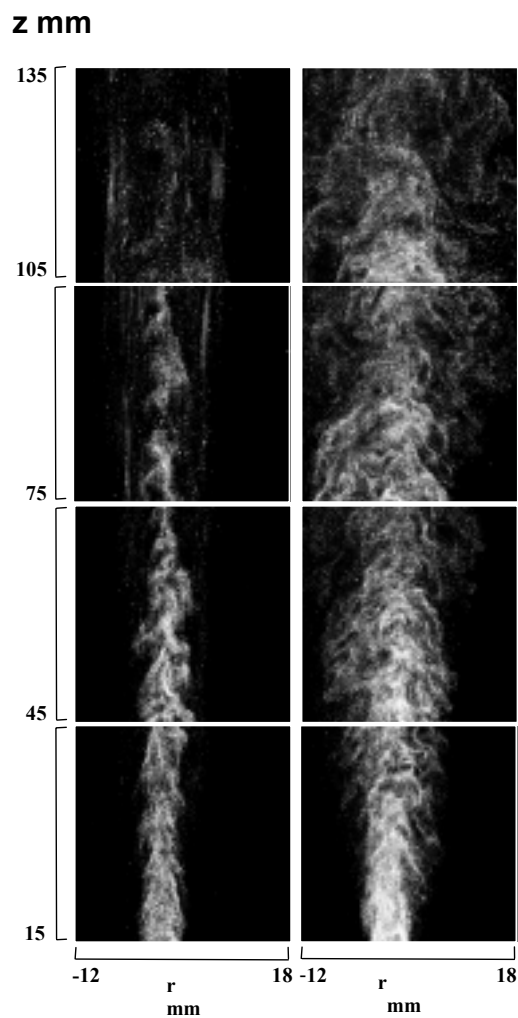


Fig. 7 Distribution of OH chemiluminescence, CH band light emission and Mie scattering intensity in z direction by MICRO

3.3 Simultaneous measurement of OH-PLIF and Mie scattering images of pulverized coal particles

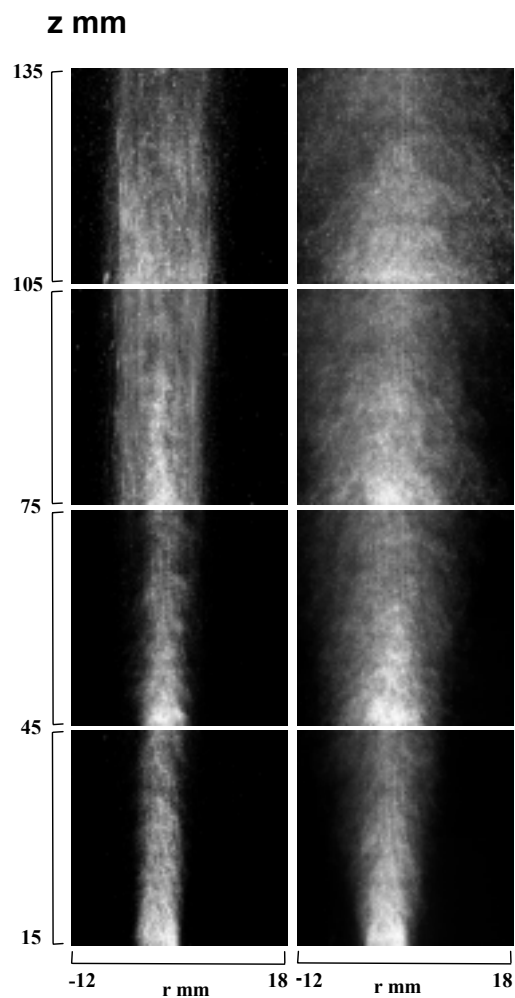
Figure 8 shows the instantaneous Mie scattering images of pulverized coal in the non-combusting case and the combusting case, obtained at 4 axial locations. The monitoring area of each image is a square of 30 mm by 30 mm as mentioned in the previous section, that corresponds to $r = -15$ to 15 mm and $z = 15$ to 45, 45 to 75, 75 to 105, 105 to 135mm. The time-averaged Mie scattering images (ten images) of pulverized coal in non-combusting case and combusting case are shown in Fig.9. These figures illustrate that particles radially spread with going downstream for both two cases. This radial spread in the non-combusting case is more apparent than that in the combusting case. This is considered as follows. The mean axial velocity of pulverized coal particles in the combusting case is faster than that in the non-combusting case due to the thermal expansion. However, the rms velocity of pulverized coal particles in the combusting case is smaller than that in the non-combusting case (Tsuji et al., 2002). Besides this, there is a high radial temperature gradient because the combustion reaction zone exists in the outer region of the flame. These are attributed to prevent the particles from moving radially.

To examine the spatial relations of combustion reaction zone and pulverized coal particles for combusting case, OH-PLIF and Mie scattering images of the particles are compared. Figure 10 shows the instantaneous OH-PLIF and Mie scattering images of the particles obtained simultaneously. In the upstream of the flame, the intensity of OH-PLIF in outer region is high due to the methane diffusion flame. Moving down stream, on the other hand, the intensity of OH-PLIF becomes high in the region where pulverized coal particles exist. What should be noted here is that the position where the high OH-PLIF intensity becomes to overlap the high particle density nearly corresponds to that where the intensities of OH chemiluminescence and CH band light emission indicate high values ($z = 80 \sim 120\text{mm}$).



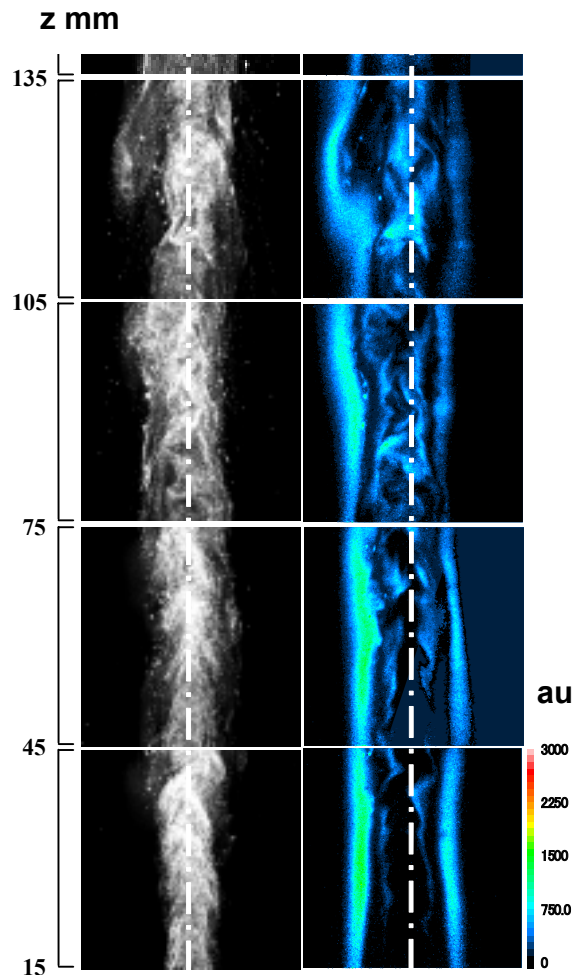
(a) combustor case (b) Non-combusting case

Fig. 8 Instantaneous Mie scattering images of pulverized coal particles



(a) combustor case (b) Non-combusting case

Fig. 9 Time-averaged Mie scattering of pulverized coal particles



(a) Mie scattering (b) OH-PLIF

Fig. 10 Simultaneous image of OH-PLIF and Mie scattering

4. CONCLUSIONS

A laboratory-scale pulverized coal combustion burner was specially fabricated, and shadow Doppler particle analyzer (SDPA) and multi-color integrated receiving optics (MICRO) were applied to the pulverized coal combustion flame. Particle velocity measurements with laser Doppler velocimetry (LDV) were carried out to discuss the accuracy of the those with SDPA. The simultaneous measurement of OH-LIF and Mie scattering image was also performed in the flame. The particle velocity by SDPA was well consistent with that by LDV. The particle velocity didn't change with particle size on the center axis. However, the particle velocity increased with particle size on the edge of the flame. The axial distributions of OH chemiluminescence, CH band light emission and Mie

scattering intensity by MICRO was reasonable. The Mie scattering images provided particle motions in the flame. The coal particles radially spread with going downstream. This radial spread in the non-combusting case is more apparent than that in the combusting case. The spatial relations of pulverized coal particles and combustion reaction zone were elucidated by the simultaneous measurement of OH-PLIF and Mie scattering image. It was found that MICRO, Mie scattering image and OH-PLIF measurement are effective for evaluating the ignition condition and characteristic of the pulverized coal combustion flames. The authors are now going not only to investigate the detailed structure of the pulverized coal combustion flame but also to use these results for the assessment of the advanced numerical simulations (Kurose et al., 2003; Akamatsu et al., 2000a; Akamatsu et al., 2000b) of the two-phase combustions.

ACKNOWLEDGMENT

The authors would like to thank Dr. Yoshihiro Deguchi of Mitsubishi Heavy Industries, Ltd. for helpful suggestions on this study.

REFERENCES

- Akamatsu, F., Wakabayashi, T., Tsushima, S., Katsuki, M., Mizutani, Y., Ikeda, Y., Kawahara, N., Nakajima, T. *Meas. Sci. Technol.* 10 (1999), pp.1240-1246.
- Akamatsu, F., Saitoh, H., Katsuki, M. *Proc. of The 8th Int. Conf. on Liquid Atomization and Spray System (ICLASS-2000)*, Pasadena, USA, (2000), pp.25-32.
- Akamatsu, F., Saitoh, H., Katsuki, M. *Proc. of The 4th KSME/JSME Thermal Eng. Conf.*, Kobe, Japan, (2000), pp.259-264.
- Deguchi, Y., Iwasaki, S. *Proc. of the 1st Asia-Pacific Conf. of Comb.*, Osaka, Japan, (1997), pp.22-25.
- Hardalupas, Y., Hishida, K., Maeda, M., Morikita, H., Taylor, A. M. K. P., Whitelaw, H. *Applied Optics* 33 (36) (1994), pp.8417-8426.
- Kurose, R., Ikeda, M., Makino, H. *Fuel* 80 (2001a), pp.1447-1455.
- Kurose, R., Ikeda, M., Makino, H. *Fuel* 80 (2001b), pp.1457-1465.
- Kurose, R., Makino, H. *Combust. Flame* 135 (2003), pp.1-16.
- Kurose, R., Makino, H., Suzuki, A. *Fuel*, 83 (2004), pp.693-703.
- Maeda, M., Morikita, H., Prassas, I., Taylor, A. M. K. P., Whitelaw, H. *Part. Syst. Charact.* 14 (1997), 79-87.
- Rothe, E. W., Andresen, P. *Applied Optics* 36 (18) (1997), pp.3971.
- Schnell, U. *Phys. Chem.* 97 (1993), pp.1582-1589.
- Tsuji, H., Kurose, R., Makino, H. *Trans. of JSME B*, 68 (2002), pp.306-312 (in Japanese)